# THE SPECTROGRAPH

## George R. Harrison Spectroscopy Laboratory
## Massachusetts Institute of Technology

## The Colour of the Sea: Sir Raman and his Effect

Maryann Fitzmaurice, MD, PhD

Associate Professor of Pathology
University Hospitals of Cleveland and Case
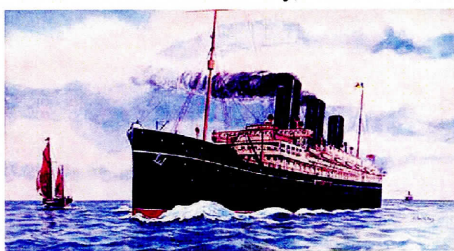Western Reserve University, Cleveland, OH



**Figure 1:** An antique postcard of the S.S. Narkunda sailing the deep blue sea.

The sea, the sky and other features of the natural world have provided inspiration for many of the great scientific discoveries of man. The world of optics is no exception. For Chandrasekhara Venkata (CV) Raman, a boy genius and Palit Chair of Physics at Calcutta University at the age of 29, it all started with the color – or rather, the colour, of the sea. Raman was making his first trip abroad by cruise ship to attend the Congress of the Universities of the British Empire in London in 1921. That trip was to be of singular importance in Raman's life and the

### Also in this issue

⊙ **Spectroscopy Laboratory News**

⊙ **Research Report:**
Low coherence probe interferometer

⊙ **Research Report:**
Single Semiconductor Nanocrystals

⊙ **Fall Seminar:**
Modern Optics and Spectroscopy

⊙ **Workshop**
Lester Wolfe Workshop

⊙ **Spectral Lines:**
Rays of the Sun

## Spectroscopy Laboratory to Get New Physical Plant

This is the second part of an article about the Spectroscopy Laboratory renovation project. The first part appeared in the Spring 2005 Spectrograph.

The Spectroscopy Laboratory will undergo a complete renovation over the next 12-18 months and acquire a new physical plant. This is part of an ambitious project to upgrade MIT's Main Group, a central set of buildings completed in the 1930's, and erect a new and unifying building for the Physics Department, the Green Center.

The Spectroscopy Laboratory will acquire new renovated research space in Building 6 of the Main Group. Through this $4 million renovation project, the Laboratory will acquire a new physical plant equipped with modern facilities. During the renovation period, which began in June, the individual laboratories of Spectroscopy Laboratory professors have been relocated to other space at the Institute, and Headquarters has been moved to MIT Building NW-14, formerly the National Magnet Laboratory.

This much needed renovation project has provided the Spectroscopy Laboratory faculty with an opportunity to define and implement future research directions. Noting that research in the Laboratory is interdisciplinary, Spectroscopy Laboratory faculty members identified four research areas that will define future research directions: ultrafast dynamics of proteins and thin films; dynamic microscopy of single cell organisms and cellular processes; biomedical optics and spectral diagnosis of disease; and combustion dynamics. In addition, a new emphasis was given to educational outreach. These programs and the prospective interconnectivity between them are addressed in the architectural design that provides high quality space for these novel research directions. The central floor plan (ground floor), shown in the figure below, reflects this vision. The 8,000 sq. ft.

## Personality
## Jeffrey Steinfeld
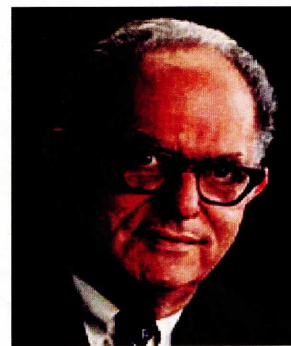


**Jeffrey Steinfeld**

Jeffrey Steinfeld first came to MIT in the late 1950's, graduating with a B.S. in Chemistry in 1962. In those bygone days, all seniors were required to carry out a senior thesis, and Prof. Steinfeld's thesis was carried out in the laboratory of Prof. Gordon Hammes, who was at that time a new assistant professor of chemistry. The work used time-resolved spectroscopy to measure reaction rates in solution using the recently invented temperature-jump technique, with a time resolution (0.1 to 500 msec) that was state-of-the-art at the time.

In graduate work in Prof. Bill Klemperer's group at Harvard University, Prof. Steinfeld used much higher spectroscopic resolution to investigate relaxation processes in molecular iodine vapor. Those experiments were carried out under steady-state conditions, with the time scale set by the radiative lifetime of $I_2^*$. The work on iodine (and an early proclivity for foreign travel) led Prof. Steinfeld to take up a post-doctoral fellowship in the laboratory of Prof. George Porter, then at Sheffield University, but soon to move on to the Royal Institution in London, a knighthood, a life peerage, and the Nobel Prize. The flash photolysis apparatus in Porter's laboratory also operated on the millisecond time scale, but Prof. Steinfeld helped set up the first laser flash photolysis (LFP) apparatus in Porter's lab which accessed the hitherto unimaginable sub-mi-

Floor plan for the renovated Spectroscopy Laboratory, ground floor of Bldg. 6. Researchers offices, probe facility and administrative offices are located on the second floor (not shown). Individual laboratories correspond to research programs of the LBRC (blue), LRF (yellow), wet chemistry and cell culture and facilities (green), and outside user facilities (purple).

---

## Spectroscopy Laboratory News
# Field Appointed Spectroscopy Laboratory Associate Director

Professor Robert Field has been appointed Associate Director of the Spectroscopy Laboratory for Scientific Coordination. He succeeds Professor Jeffery Steinfeld, who has held this post for the past 25 years.

Professor Michael Feld, Spectroscopy Laboratory Director, said that Professor Steinfeld has played a crucial role in the evolution of the Spectroscopy Laboratory into the era of modern spectroscopy, and that his coordination of the research activities fo the NSF funded Laser Research Facility (LRF) has been a great success. Dr. Ramachandra Dasari will continue as Associate Director.

Prof. Steinfeld began his research at the Spectroscopy Laboratory in the 1960's, obtaining the first laser induced molecular fluorescence in iodine using an argon ion laser. He also rejuvenated the use of the echelle spectrograph in order to assign $I_2$ excited levels pumped by various laser and atomic resonance lamp sources.

Among his major contributions have been the development of infrared double resonance (IRDR) spectroscopy using a $CO_2$ laser pump and a tunable diode laser probe, with which he obtained kinetic data on several physical and chemical systems. The IRDR experiments in ozone and methane brought Prof. Steinfeld into atmospheric science community and recently his efforts are devoted to issues related to energy and atmosphere chemistry.

Professor Field, like Prof. Steinfeld, is a physical chemist, with special interest in small molecule structure and dynamics. He has led a large research group in the Laboratory and has made important contributions in the area of highly excited vibrational states of molecules.

Professor Field's contributions to the Laboratory began when he arrived in the late 1970's and received the first Tunable Laser Facility grant from NSF (1977). This led to a very important research technique, Stimulated Emission Pumping, which he successfully used for more than two decades studying formaldehyde and acetylene.

As Associate Director for Scientific Coordination, Prof. Field will assume Prof. Steinfeld's duties, including coordinating the scientific activities of the LRF. ✳

---

*Physical plant, continued from page 1*

research space features 14 laboratories, a probe fabrication facility (second floor, not shown) and wet laboratories for small-scale chemical synthesis, cell culture and

tissue processing. Individual laboratories will be equipped with modern utilities and have been designed to meet the specifications of the individual research groups. The addition of a separate laboratory for cell culture represents the emphasis on cellular biology in all aspects of the current technical program. Located on the second floor adjacent to the main offices, the probe fabrication facility is designed to have a near 'clean room' air quality, important for the assembly of optical fiber probes used in the biomedical research. In addition, outside investigators will have access to a Raman microscopy laboratory with continuous excitation wavelengths available between 600–1000 nm and a time-resolved fluorescence instrument based on an amplified fs Ti:sapphire system and streak camera. ✳



A model shows sunlit walkways connecting Building 6 with the planned new structure. Image courtesy Payette Associates.

crosecond regime.

Those initial LFP experiments resulted in the first reported example of a multiphoton ssociation process. On a return visit to the Royal Institution, it was quite a surprise to see that LFP apparatus displayed in the "ambulatory gallery" along with Faraday's first generator (since removed to the Faraday museum, admission £l), Dewar's first flask, and Bragg's first diffraction apparatus.

Returning to MIT as an assistant professor in 1966, Prof. Steinfeld continued to develop the theme of obtaining kinetic data on physical and chemical systems using time-resolved spectroscopy. Combining a $CO_2$ laser pump with a tunable solid-state diode laser (TDL) probe led to the development of infrared double-resonance (IRDR) spectroscopy, which was extensively employed in Prof. Steinfeld's laboratory and elsewhere. The time resolution of such an IRDR experiment was still in the microsecond range, but this was sufficient to resolve single-collision events in dilute gases. Among the systems initially investigated was $SF_6$ (at that time a euphemism for $UF_6$), which conveniently had strong absorption bands at $CO_2$ laser output frequencies.

The IRDR measurements on ozone were reatly successful, filling some major gaps in the spectroscopic database. These experiments brought Prof. Steinfeld into contact with the atmospheric science community and the NASA Upper Atmosphere Research Program, where he learned that similar gaps existed in the data base for methane (which turns out to be a major greenhouse gas). Using $CO_2$ lasers, however, strongly limited the range of molecules which could be investigated using IRDR, and so a series of surrogates were studied including $^{13}CD_4$, silane, and $CHD_3$-a strategy known as "tuning the molecule to the laser". While a great deal of interesting information about spherical and near-spherical top molecules came out of these measurements, this was still not "real" methane, i.e. $CH_4$.

It finally became possibly to study $CH_4$ using newly available equipment in the Harrison Spectroscopy Laboratory, namely a Raman-shifted Ti:sapphire pump laser with improved TDL probes.

At about the same time, Prof. Steinfeld became increasingly aware of another set changes that were being observed in the abundances of atmospheric gases such as methane, as well as ozone, carbon dioxide, and others. An example of such change is shown in Fig. 1.
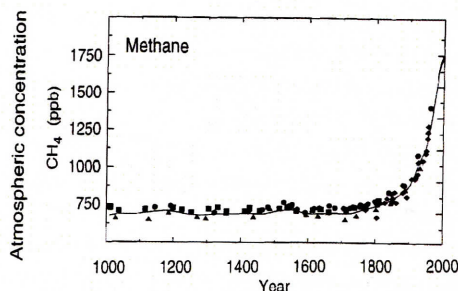


**Figure 1**: An example of human impact on the abundance of atmospheric gases. The increase of methane gas during the last millenium is shown.

The time scale here is not milliseconds or microseconds (or even picoseconds or femtoseconds!) but a thousand years - about 12 orders of magnitude longer time scale than the IRDR measurement shown above. The "perturbation" is not a laser or other controlled laboratory scenario, but human activities such as agriculture (particularly rice and cattle cultivation), natural gas extraction and distribution, and dumping trash into landfills. And the induced change is not relaxing to its pre-perturbation level, but is continuing to diverge from its "pre-industrial" level.

Professor Steinfeld views this observation as emblematic of a whole set of changes with time that are altering the natural environment - the Earth System - which is the system in which we all live and which is, in fact, the basis of all the social, technological and economic systems on which we depend.

Professor Steinfeld has great concerns about changes in the earth's atmosphere. He writes as follows:
"In my own lifetime,
- the carbon dioxide content of the Earth's atmosphere has increased by ~23%;
- the global average surface temperature and the mean sea level have both measurably increased;
- the rate of species extinction has accelerated and the level of biodiversity correspondingly decreased;
- half the oil that ever existed has been extracted and used up - by being burned;
- the total human population has tripled, with a fifth of that total living in poverty.

While academics continue to debate the issues of sustainability and sustainable development, one thing is certain - the trends enumerated above are not in any sense sustainable. Our descendants, and the students now in our classrooms and laboratories, will be pursuing their careers, raising their own families, and just trying to survive in a world that may be increasingly subject to climate extremes, shortages of food and disappearing sources of cheap and easily available energy, and the social unrest that will follow as a result. For all their sakes, we have an absolute obligation to try to understand what is happening to the world that we inhabit, to develop strategies to mitigate against adverse trends, and most importantly to educate the next generation about these issues. We owe them no less." ☀

## Spectroscopy Laboratory News
# Field to Receive Bomem-Michelson Award

Robert Field, the Haslam and Dewey Professor of Chemistry at MIT and newly appointed Associate Director of the Spectroscopy Laboratory, has been selected as the 2006 recipient of the Bomem-Michelson Award of the Coblentz Society. The award will be presented at the March meeting of Pittcon '06 in Orlando Florida.

Dr. Field is being cited for his work in molecular spectroscopy. This includes contributions in the areas of molecules in vibrationally highly excited states, the spectra and electron-nuclear coupling dynamics encoded in Rydberg spectra, and the theory of spectroscopic perturbations.

Field, a physical chemist, has a special interest in small molecule structure and dynamics. Over the years he has developed techniques such as Microwave-Optical and Optical-Optical Double Resonance Spectroscopy, Stimulated Emission Pumping, Frequency Modulatation Enhanced Magnetic Rotation Spectroscopy, and Extended Cross Correlation Spectroscopy, and used them to reveal extremely large amplitude motions along the minimum energy isomerization path in acetylene, bond-breaking isomerization in HCP, and the first complete all-states, all-dynamics characterization of a molecule (CaF). One exciting finding has been the observation of ergodic dynamics in a fully rotationally assignable spectrum of acetylene, in particular the energetic coexistence of ergodic vibrational dynamics in the first excited triplet state and regular dynamics in the third excited state of acetylene.

The Bomem-Michelson Award of the Coblentz Society is awarded annually to a scientist who has advanced the experimental and conceptual frontiers of molecular spectroscopy. Past recipients include Carl Lineberger, William Klemperer (Field's PhD supervisor), Richard Saykally, Herbert Strauss, Terry Miller, and Daniel Neumark. ☀

# Low coherence probe interferometer for measuring surface profiles and motion in biology

Christopher Fang-Yen, Mark C. Chu, H. Sebastian Seung*, Ramachandra R. Dasari and Michael S. Feld

G. R. Harrison Spectroscopy Laboratory, *Howard Hughes Medical Institute and Department of Brain and Cognitive Sciences, MIT.

Several biomedical imaging techniques are based on the interference of light. In phase contrast microscopy [1] and differential interference contrast [2] (DIC) microscopy, optical phase shifts induced by a sample are converted to intensity differences in the magnified image. Such techniques are essential for live cell imaging, since most unstained cells are nearly invisible under brightfield illumination.

Interferometry using broadband (low coherence) sources can be used to perform depth-resolved reflectivity measurements in a sample. In optical coherence tomography (OCT), [3] the optical analogue of ultrasound imaging, a low coherence Michelson interferometer with a scanning reference arm produces 2D and 3D images of tissue structures, with a transverse and longitudinal resolution of several microns.

Recently, a number of low coherence interferometers [4-7] have been developed to perform high resolution phase measurements of light reflected from biological samples, allowing the detection of motions on the scale of nanometers or smaller. The interferometers measure the phase of light scattered from a sample relative to a reflection from a nearby reference surface on the same optical path. This nearly common-path configuration (referred to here as phase-referenced interferometry) can be used to strongly reduce phase noise due to external perturbations. Studies based on two-wavelength interferometry [4] and spectral domain interferometry [5] have been used to measure motions in cultured cells; in these experiments the reference beam was provided by reflection from the bottom of the coverslip on which the cells were attached. In phase-referenced dual-beam [6] and polarization-dependent [7] low coherence interferometers, reference surfaces were positioned above the samples to measure nanometer-scale surface displacements in nerves during the action potential [8].

Two aspects of phase-referenced interferometry may be problematic in some situations. First, it requires a reference surface to be in reasonably close proximity to the sample of interest and aligned to reflect the incident beam back to the interferometer optics. In many situations such a configuration may be difficult or inconvenient to achieve. Space for the reference surface may be limited, and the reference surface may impede access to the sample. The reference surface may need to be adjusted in position and/or angle if more than one point on the sample is to be investigated, or if the sample changes position or orientation significantly during the experiment. Therefore it would be desirable to have a system in which no separate reference surface is required.

A second difficulty is a limitation in numerical aperture (NA) of the light delivery and collection optics due to the axial separation between sample and reference. High NA may be desirable to obtain very small transverse focus size and for optical sectioning in three-dimensional samples by confocal imaging. For a high-NA beam with approximately spherical wavefront converging onto the sample, reflections from sample and reference have apparent source locations separated by roughly twice the distance between sample and reference surface. For sample and reference surfaces to be simultaneously in focus, their separation must be on the order of the depth of field $\sim l/NA^2$ or smaller. This requirement is clearly difficult to meet for NA$\sim$1.

We have designed a phase-referenced interferometer in which the reference field is created by a Fresnel reflection from a cleaved fiber tip located inside a small optical fiber probe. Light transmitted by the fiber is focused onto the sample through a gradient index (GRIN) microlens. By integrating the reference reflection into the probe, a separate reference surface is no longer required. Furthermore, the NA of the system is limited only by the NA of the focusing lens, allowing a transverse spot size at focus comparable to the wavelength of light used.

Our interferometer (Fig. 1) resembles the design presented in Ref. 6. Broadband light from a superluminescent diode (Superlum SLD-761, center wavelength 1549 nm, FWHM bandwidth 49 nm) enters a Michelson interferometer containing acousto-optic modulators driven at frequencies $\omega_1 = 110.05$ MHz and $\omega_2 = 110$ MHz, each aligned in a double-pass configuration. The outputs from the two ports of the interferometer are routed via optical circulators to the probe (Fig. 2) and a reference gap composed of two glass windows separated by an adjustable distance. Reflected light from these elements are detected by two AC-coupled photodetectors.

Optics are adjusted so that the following optical path delays are equal to well within the coherence length: (i) $\Delta L$, between the two Michelson interferometer arms; (ii) $\Delta L_S$, between the sample reflection and probe fiber reflection; and (iii) $\Delta L_R$ between the two reflections from the reference gap. The photodetectors then record heterodyne signals at frequency $\Omega = 2(\omega_1 - \omega_2) = 100$ kHz. The photodetector outputs are digitized by a 12-bit A/D card (National Instruments PCI-6110) and a computer calculates the phase difference $\Delta\phi(t)$ between the two signals. The phase difference $\Delta\phi(t) = k_0 (\Delta L_S - \Delta L_R)$, where $k_0$ is the peak wave number of the source, represents the phase of the sample reflection relative to the probe reference reflection, assuming a time-independent reference gap. The phase shift can then be expressed as a displacement $\Delta d(t) = \Delta\phi(t)/2 k_0$.

The probe (Fig. 2) was constructed as follows. A single mode optical fiber was stripped and cleaved at a right angle using a fiber cleaver so that a backreflection of about 3% was achieved. The cleaved fiber end was inserted into a 2.8mm diameter glass ferrule. Cylindrical aluminum housings positioned the ferrule and a 0.29-pitch GRIN lens (Newport LGI1560, 0.46 NA) as shown. The distance between the fiber tip and interior face of the GRIN lens is
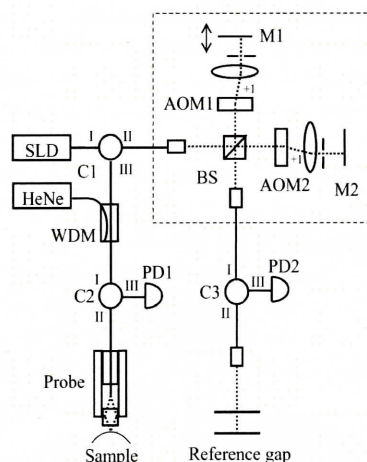


**Figure 1**: Phase-referenced probe interferometer setup. Dashed box indicates Michelson interferometer. SLD: superluminescent diode; AOM1, AOM2: acousto-optic modulators, M1, M2: mirrors; C1-C3: optical circulators; BS: beamsplitter; PD1-PD2: photodetectors, HeNe: guide laser, WDM: wavelength division multiplexer.

approximately 4 mm; the working distance (WD) between the tip of the GRIN lens and the focus is 0.5 mm. The focus spot diameter is estimated to be ~ 2μm FWHM.

To test probe stability, we mounted the probe in a cage plate assembly (Thorlabs)
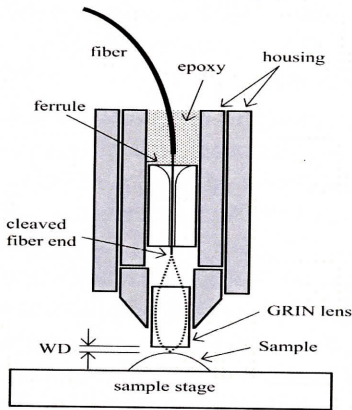


**Figure 2**: Detail of probe assembly. WD: working distance, approximately 0.5 mm.
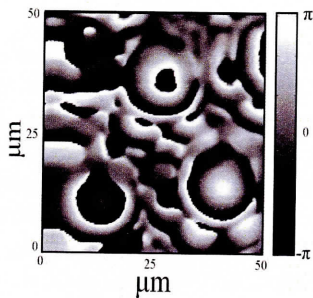


**Figure 3**: Phase image from compound eye of a fly, showing three facets. Pixel size 0.33 x 0.33 μm.

with a fixed glass surface positioned at the sample focus. With a probe output power of 200 mW, the total noise between 1 Hz and 1 kHz was approximately 0.2 mrad (rms), corresponding to a displacement of 0.2 angstroms.

For the imaging experiments, samples were raster scanned under the fixed probe by means of an XY translation stage with motorized actuators. We first imaged the spherical surface of a plano-convex lens (focal length 75 mm) to confirm the accuracy of the phase measurements. A 400 μm long cross section of the phase map through the center of the lens was phase unwrapped to remove 2π-ambiguity. The measured radius of curvature (ROC) of 37.1 ± 1.5 mm determined by a quadratic fit to the resulting height profile was in agreement with the lens manufacturer specified ROC of 38.6 ± 0.5 mm.

To demonstrate the biological imaging capabilities of the probe, we used the probe to image a small region from the compound
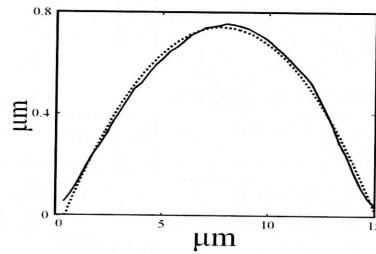


**Figure 4**: Solid line: cross section of single fly eye facet (lower left in Fig. 3). Dashed line: fit to y =ax2+bx+c, with a = -0.00136 (μm)-1, b = 0.203, c = 0.0114 μm.
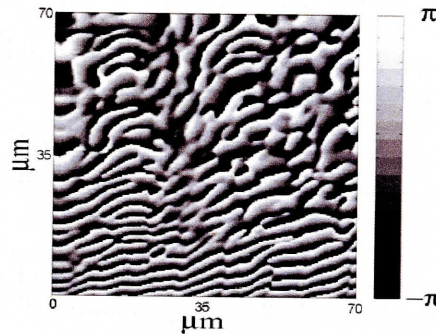


**Figure 5**: Reflection phase image of a ctenoid fish scale from Lutjanus campechanus.

eye of a housefly (*Musca domestica*). The outer surface of the compound eye is composed of a hexagonal lattice of facets, which are front lens surfaces of the ommatidia, cone-shaped structures for light collection and detection. For our images, a portion of the fly's compound eye was dissected and mounted on the translation stage to present a surface approximately perpendicular to the probe beam. The probe position was adjusted to maximize the reflected power at the center of facets (peak reflectivity ~10%). Figure 3 shows a scanned-sample phase map of a 50 x 50 micron region. Ring patterns corresponding to three circular facets are visible. A cross section of a single facet was phase unwrapped to remove 2π-ambiguity and converted to a distance. The resulting profile is shown in Fig. 4 with a best-fit second order polynomial. The curvature at the center of the parabola corresponds to an ROC of 36.8 microns.

In Fig. 5 we show a reflection phase image of a ctenoid fish scale from a red snapper (*Lutjanus campechanus*), imaged via a similar scanning procedure. Ridges in the scale are seen as vertical modulations in the fringe patterns.

Data acquisition rate in this experiment was limited by the stage to approximately 10 pixels/second. In future work, the imaging speed will be increased to ~1000 pixels/sec with probe scanning using a piezo translator.

To demonstrate the probe interferometer's ability to measure small, rapid motions, we used it to measure nanometer-scale surface displacements in a lobster nerve during the action potential. These mechanical displacements, which have been attributed to rapid water influx into axons, have been observed in a number of invertebrate and vertebrate nerve preparations [8].

The walking leg nerve (~1 mm diameter, ~50 mm long) from an American lobster (*Homarus americanus*) was dissected and placed on an acrylic nerve chamber. The chamber contains five wells filled with a saline solution. Between wells the nerve is surrounded by an insulating layer of petroleum jelly to maximize inter-well resistance. A compound action potential is generated by a current pulse from a stimulus isolator and is detected at the other end by an amplifier with gain 10⁴. The probe is aligned such that the beam reflects from the top of the nerve surface. The probe, translation stage, and nerve chamber were integrated into a cage plate assembly (Thorlabs) for high mechanical stability. Figure 6 shows a typical result for the simultaneous electrical potential and optically measured displacement of a nerve. The spike at time zero in the electrical signal is a stimulus artifact. It is followed by peaks corresponding to action potentials of axons in the nerve bundle; the number and shape
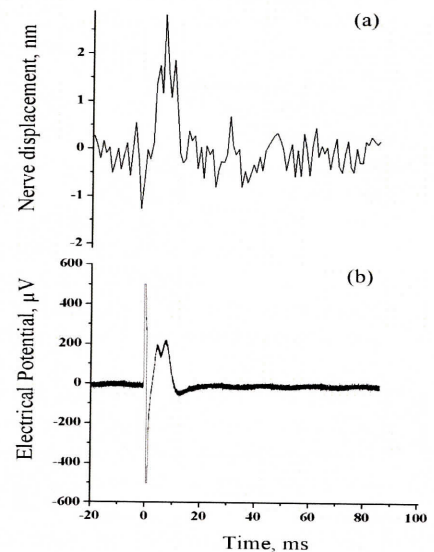
**Figure 6**: (a) Interferometric measurement of nerve displacement using probe and (b) simultaneous electrophysiological measurement. Single shot data (no signal averaging). Stimulus current 8 mA; stimulus duration 1 ms. The electrical signal spike at 0 ms is a stimulus artifact. The displacement signal is low-pass filtered at 1 kHz. A linear component with negative slope ~300 nm/sec, due to drying of nerve, was subtracted from the signal in (a).

of peaks varied from sample to sample. The optical signal shows a peak of height ~3 nm and FWHM duration ~10 ms, with a direction corresponding to an upward displacement. Amplitude and duration of displacements measured during the action potential were comparable to those observed earlier [6].

The high transverse resolution of the phase-referenced probe interferometer will allow its use in the measurement of cell membrane displacements in single axons, single neurons, and other cells. The probe may also find applications as an optical fiber sensor [10] for displacement, vibration, or sound.

## References

1. F. Zernike, "How I discovered phase contrast", Science 121, 345-349 (1955).
2. G. Nomarski and A. R. Weil, Revue de Metallurgie 52, 121 (1995) .
3. D. Huang, E. A. Swanson, C. P. Lin, J. S. Schuman, W. G. Stinson, W.Chang, M. R. Hee, T. Flotte, K. Gregory, C. A. Puliafito, and J. G. Fujimoto, "Optical Coherence Tomography", *Science* 254, 1178-1181 (1991).
4. C. Yang, A. Wax, M. S. Hahn, K. Badizadegan, R. R. Dasari, and M. S. Feld, "A phase-referenced interferometer with sub-wavelength and sub-Hertz sensitivity applied to the study of cell membrane dynamics," Opt. Lett. 26, 1271-1273 (2001)
5. M. A. Choma, A. K. Ellerbee, C. Yang, T. L. Creazzo, and J. A. Izatt, "Spectral-domain phase microscopy", Optics Letters 30, 1162-1164 (2005).
6. C. Fang-Yen, M. Chu, H. S. Seung, R. R. Dasari, and M. S. Feld, "Non-contact measurement of nerve displacement during action potential with a dual-beam low coherence interferometer", Optics Letters 17, 2028 (2004).
7. T. Akkin, D. P. Dave, T. E. Milner, and H. G. Rylander, "Detection of neural activity using phase-sensitive optical low-coherence reflectometry", Optics Express 12, 2377-2386 (2004).
8. I. Tasaki, "A Macromolecular Approach to Excitation Phenomena: Mechanical and thermal changes in nerve during excitation," Physiol. Chem. Phys. Med. NMR. 20(4):251-68 (1998).
9. A. Watanabe, "Change in optical activity of a lobster nerve associated with excitation", J. Physiol. 389, 223-253 (1987).
10. B. Lee, "Review of the present status of optical fiber sensors", Optical Fiber Technology 9, 57-79 (2003).

field of optics.

Raman had spent much of his career leading up to this trip studying vibrational and acoustical effects of various kinds. Some of his earliest work was in acoustics, including studies of the complex vibrations and overtones of the violin and several Indian classical string and percussion instruments [1]. During his stay in London, Raman visited St. Paul's Cathedral and was fascinated by another acoustic phenomenon, the whispering gallery, a circular gallery at the base of St. Paul's great dome, where a whisper on one side carries around the dome and can be heard on the opposite side some 43 meters away. Before he left London, Raman had published one of the first of his many letters to *Nature* [2], explaining the phenomenon and refuting an earlier theory put forward by Lord Rayleigh, 1904 Nobel Laureate in Physics. This simple tourist encounter is at least in part responsible for the whispering gallery mode lasers in use today.

Raman traveled to and from England by sea, and it is said that he sat for hours on the upper deck of the ocean liner staring at the deep blue color of the Mediterranean. Like the whispering gallery, it peaked his scientific curiosity. During the voyage, Raman conducted experiments peering into the depths of the sea using the Nicol (calcium calcite polarization) prism he always carried, and sent a second letter to *Nature* entitled "The Colour of the Sea" [3] by telegraph before even setting foot on dry land, from the S.S. Narkunda (Fig. 1) in Bombay Harbour on September 26, 1921.

Rayleigh had proposed that the blue color of the sea was due to reflected sky light and absorption by matter suspended in the water [4]. Raman's experiments clearly showed that the blue color of the sea was independent of reflection and absorption and due instead to molecular diffraction, most likely from water molecules themselves. These simple experiments conducted at sea led Raman to pursue more detailed studies of the scattering of light once back home in Calcutta, and ultimately to discover the vibrational effect that would come to bear his name.

In 1923, Arthur Compton proved the concept put forward by Planck and Einstein that radiation is not only wave-like, but also particle-like in nature. When a beam of radiation traverses an atom, most of the radiation is elastically scattered and therefore of unchanged wavelength. Using a graphite target, Compton had shown that a small fraction of the radiation emerged in directions other than that of the incident beam due to inelastic scattering of the x-rays by electrons [5]. This came to be called the Compton effect (for which he received the Nobel Prize in Physics in 1927). Inspired by Compton's discovery, Smekal predicted that photons should likewise be inelastically scattered by vibrational transitions within molecules [6].

Raman and his colleagues at The University of Calcutta and Indian Association for the Cultivation of Science set out to prove Smekal right. We now know that one of the characteristics of inelastic scattering is that its intensity scales as the fourth power of the energy. This meant that the inelastic scattering effect Raman sought using visible light (~500nm) was at least 10 orders of magnitude weaker than that observed by Compton using x-rays (0.7 nm). Raman was able to observe this weak effect by using the most intense light source available at the time, the sun. In his initial experiments, Raman used a 7-inch reflecting telescope in combination with a short focal length eyepiece to focus sunlight onto a purified (distilled) liquid or its dust-free vapor. He then used complementary yellow-green and blue-violet filters to observe the incident and scattered beam of light. Using this amazingly simple experimental apparatus, Raman discovered that a small amount of the incident light had been inelastically scattered by the molecules in the liquid and shifted in energy into another part of the spectrum. This shift in wavelength, he later observed as additional bands on a spectrograph (Fig. 2).

This remarkable discovery was made on Monday February 27, 1928 and described by KS Krishnan, Raman's student, in his diary:

*"Went to the Association in the afternoon. Professor was there. Started studying the effect of incident light wavelength on the new scattering effect. Astonished to see that the scattered radiation has wavelength different from the incident one - wavelength higher and shorter than that of the incident radiation. [7]"*

Raman didn't waste any time and that Friday, March 3, 1928, he and Krishnan published another letter in *Nature* entitled "A New Type of Secondary Radiation" describing what would ultimately come to be called the Raman effect or Raman shift [8].

There was good reason for Raman to hurry, as he was in danger of being scooped. As

# Seminar on
# Modern Optics and Spectroscopy

## Fall Semester 2005

---

**October 11**      Junichiro Kono, Rice University
**Ultrafast and magneto-optical spectroscopy of carbon nanotubes**

**October 25**      Gary Wiederrecht, Argon National Laboratory
**Optical spectroscopy of nanoscale plasmonic heterostructures**

**November 1**      Subra Suresh, MIT
**Nanotechnology and computations at the intersections of engineering, biology and medicine**

**November 8**      John Thomas, Duke University
**Atomic Fermi gases with strong interactions:  Superconductors, neutron stars, and quark gluon plasmas on a desktop**

**November 15**      Stephanie Reich, MIT
**Single-walled carbon nanotubes - tuning the optical properties of a nanomaterial**

**November 29**      Lene Hau, Harvard University
**Shocking Bose-Einstein condensates with slow light**

**December 6**      Joel Parks, Roland Institute at Harvard
**Ultrafast imaging and control of plasma waves in Fermi seas**

**December 13**      Yoel Fink, MIT
**Can invisible objects see?  On the imaging properties of transparent photodetecting fiber webs**

**Tuesdays, 12:00 - 1:00 p.m., Grier Room (34-401A)**
Refreshments served following the seminar.

---

# Lester Wolfe Workshop in Laser Biomedicine

# Nanoparticles in biomedicine: Let there be light!

Tuesday, November 15, 2005. 4:00-6:00 PM
Grier Room, 34-401
EG&G Education Center, MIT
50 Vassar Street, Cambridge

---

In recent years there has been an explosion in research on biomedical applications of nanoparticles. This workshop will explore the role of optics and photonics in this interdisciplinary field. Topics include gold nanoparticles for cancer diagnosis and therapy, fluorescent quantum dots for imaging disease, and novel approaches to drug delivery and tissue engineering.

---

**All that glitters is gold: Potential *in vitro* and *in vivo* biomedical applications of noble metal nanoparticles**

*Ivan El-Sayed, University of California at San Francisco*

**Designing quantum dots for fluorescence based biomedical applications**

*Moungi Bawendi, MIT*

**High throughput approaches to drug delivery and tissue engineering**

*Daniel Anderson, MIT*

Refreshments served at 3:30 pm

---

early as 1913, two Russians, Mendelsram and Landsberg, had been conducting studies similar to those of Raman. In 1925 they began such studies using quartz crystals rather than the dustless gases and liquids being studied by Raman. But it was not until 1928, the same year as Raman made his seminal discovery, that the Russian pair obtained quartz crystals pure enough to observe the inelastic scattering effect in question. In fact, records show that they made their first observation of the "Raman effect" on February 21, 1928, six days before Raman. However, unlike Raman, they did not immediately publish their observation but rather presented it to a meeting of the Russian Academy at which, reportedly, no one believed them. Disheartened, they did not publish their observations until after Raman had published his[10].

There was also danger of being scooped right here in the U.S. According to Michael Feld, Director of the G.R. Harrison Spectroscopy Laboratory, RW Wood at Johns Hopkins University was a colleague of Raman's. As soon as Raman observed the effect, he sent a telegram to Wood. Wood rushed into his well-equipped laboratory and repeated Raman's results in a matter of hours, and then sent off his own letter to *Nature*. Wisely, however, Raman had submitted his letter to Nature by telegram at the same time he wrote Wood. [11]. Hence Raman received first priority.

There are a number of remarkable things about Raman's letter to Nature. First is its brevity, just 368 words. The second is the speed with which it was published, just 5 days after the effect was observed, a feat that may never be equaled again, even in the era of on-line journal publication. But Raman had not really waited 5 days to report his discovery. Ahead of his time, he rushed to take advantage of the 24-hour news cycle and contacted the Associated Press of India. A news report of his discovery was printed the very next day [9]. The third remarkable thing about that third letter to *Nature* is the amount of work Raman and Krishnan accomplished in those 5 days.

"Some sixty different common liquids have been examined in this way, and every one of them showed the effect in greater or lesser degree" [8].

By August of the following year there were already 150 scientific publications related to the Raman effect [12]. That year, 1929, CV Raman was nominated for the Nobel Prize in Physics. But the prize went instead to



**Figure 2:** CV Raman with spectrograph, Raman tube and first Raman spectra photographed.

Louis de Broglie for his work on the wave nature of the electron. Raman was nominated again in 1930 and, just 2 years after his initial experiments, was awarded the Nobel Prize in Physics at the age of 42.

One might think that the importance of Raman's trip aboard on an ocean liner in the Mediterranean Sea to the discovery of vibrational light scattering has been exaggerated. However, when King Gustav V of Sweden awarded Raman his Nobel Prize on December 11, 1930, Raman began his Nobel lecture on "The Molecular Scattering of Light" with an introduction he entitled "The colour of the sea". In it he said:

*In the history of science, we often find that the study of some natural phenomenon has been the starting point in the development of a new branch of knowledge. We have an instance of this in the colour of skylight, which has inspired numerous optical investigations, and the explanation of which, proposed by the late Lord Rayleigh, and subsequently verified by observation, forms the beginning of our knowledge of the subject of this lecture. Even more striking, though not so familiar to all, is the colour exhibited by oceanic waters. A voyage to Europe in the summer of 1921 gave me the first opportunity of observing the wonderful blue opalescence of the Mediterranean Sea. It seemed not unlikely that the phenomenon owed its origin to the scattering of sunlight by the molecules of the water. To test this explanation, it appeared desirable to ascertain the laws governing the diffusion of light in liquids, and experiments with this object were started immediately on my return to Calcutta in September 1921. It soon became evident, however, that the subject possessed a significance extending far beyond the*

*special purpose for which the work was undertaken, and that it offered unlimited scope for research. It seemed indeed that the study of light-scattering might carry one into the deepest problems of physics and chemistry...* [13].

And so, a pivotal advance in the field of optics came from something as ordinary and yet as extraordinary as the "colour" of the sea.

Raman spectroscopy quickly became the technique of choice for conducting molecular vibrational studies in both research and industry. However, after World War II, it fell out of favor and was largely replaced by then simpler infrared and near infrared spectroscopy techniques. Like the technique it inspired, the SS Narkunda also fell on bad times and was sunk by the German Luftwaffe in 1942 when pressed into use as a troop carrier in World War II.

Fortunately, in the 1960's the advent of lasers brought renewed interest in stimulated Raman scattering. And more recent instrumentation advances including back-thinned, liquid nitrogen cooled CCD detectors have once again brought CV Raman and his "effect" to the scientific forefront. The Raman spectra we analyze today using this advanced instrumentation (Fig. 3) look little like the bands Raman and Krishnan first saw in their laboratory at 210 Bow Bazaar Street in Calcutta. The Raman bands in these modern spectra represent a chemical fingerprint of the molecular species examined.

And, while the renaissance of Raman spectroscopy had its first biomedical impact in the fields of biochemistry and biophysics, where it was used for key chemical and structural studies of DNA, lipid membranes, hemoglobin and enzymes such as the cytochrome oxidases, perhaps its greatest impact will be in clinical medicine. Raman spec-
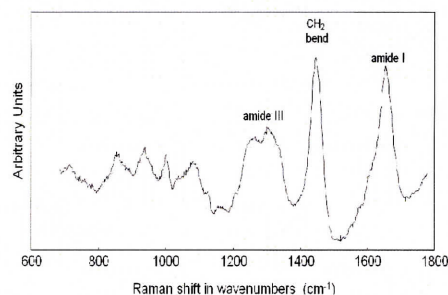
**Figure 3:** Raman spectrum of invasive breast cancer in human breast tissue obtained with Ti-sapphire laser excitation light at 830nm and back-thinned, liquid nitrogen cooled CCD detector. Bands assigned to CH2 bend, amide I and amide III molecular vibrations are shown.

troscopy is now being used to probe intact living cells, tissues and even humans. In fact, Raman spectroscopy techniques are currently being developed at the MIT Laser Biomedical Research Center at the G.R. Harrison Spectroscopy Laboratory for painless transcutaneous monitoring of blood glucose in diabetics [14], identification of vulnerable atherosclerotic plaques in the coronary arteries of patients at risk for heart attacks [15], and the real time *in vivo* diagnosis of breast cancer [16]. ✳

## References

1.  C.V. Raman, *Bulletins of the Indian Association for the Cultivation of Science* 6, 11 and 15, 1918.
2.  C.V. Raman: Whispering-Gallery phenomena at St. Paul's Cathedral. *Nature* 108:42, 1921.
3.  C.V. Raman: The colour of the sea. *Nature* 108: 367, 1921.
4.  J.W. Rayleigh: On the light from the sky. *Phil. Mag.* 41:107-120, 274-279, 1871.
5.  A.H. Compton: A quantum theory of the scattering of x-rays by light elements. *Phys. Rev.* 21:483,1923.
6.  A. Smekal: Zur quantentheorie der dispersion. *Naturwissenschaften* 11: 873 (1923).
7.  V. P. N. Nampoori: A co-traveler of light, colour and beauty: Life and work of C.V. Raman. http://www.photonics.cusat. edu/Article5.html.
8.  C. V. Raman and K. S. Krishnan: A new type of secondary radiation. *Nature* 121: 501-502, 1928.
9.  C.V. Raman: A new radiation. *Indian Journal of Physics*, March 31,1928.
10. Mendelsram and Landsberg Nature (Naturwissenschaften (1928, 16, 557)) April and May 1928.
11. personal communication.
12. R. Singh and F. Riess: Sir C. V. Raman and the story of the Nobel Prize. http://www. iisc.ernet.in/~currsci/nov10/articles33. htm.
13. C. V. Raman: The molecular scattering of light. Nobel Lecture, December 11, 1930. Nobel Lectures. Physics 1922-1941, Elsevier Publishing Company, Amsterdam, 1965. http://nobelprize.org/physics/laureates/1930/raman-lecture.pdf.
14. A.M.K. Enejder, T.W. Koo, J. Oh, M. Hunter, S. Sasic, M.S. Feld and G.L. Horowitz: **Bloo**d analysis by Raman spectro scopy. *Optics Letters* 27: 2004, 2002.
15. H.P. Buschman, J.T. Motz, G. Deinum, T.J. Romer, M. Fitzmaurice, J.R. Kramer, A. van der Laarse, A.V. Bruschke and M.S. Feld: Diagnosis of human coronary atherosclerosis by morphology-based Raman spectroscopy. *Cardiovascular Pathology*, 10(2): 59-68, 2001

## Spectral Lines
## Rays of the Sun

by Stephen R. Wilk

I sometimes think that we should spend at least a little time explaining everyday manifestations of physics to undergraduates, so that they can talk about phenomena that appear in everyday lives. Everyone studies electricity and magnetism, usually in their freshman year, but even advanced courses don't discuss the most familiar form of magnetism – ferromagnetism -- at all. It's brushed aside, hidden under a rug, because it doesn't fit neatly into the lesson plan. The Freshman-home-on-spring-break has to excuse himself, saying that they haven't covered the topic yet. Most, in fact, are never exposed to it.

Similarly, it has always seemed odd to me that probably the most familiar optical phenomenon is never addressed. It's probably one of the first thing we take notice of when we make our own survey of the optical world – the rays of the sun [1]. The same image of a round solar disc surrounded by straight rays appears in Akhenaton's Egypt, 3500 years ago [2]. The rays of the sun literally fill the sky in Pieter Breughel the Elder's 1570 print Summer [3]. But, in all my years in college studying and teaching optics, no one has ever addressed this phenomenon. Just what does cause solar rays?

"Scattering by dust" answered a colleague when I posed the question to him. But let's be clear about the phenomenon under discussion. I'm not referring to the shafts of sunlight breaking through clouds, creating relatively broad sunbeams which can be easily photographed [4]. Jearl D. Walker calls these the "Rays of Buddha" [5], and they are certainly due to the sun's rays being scattered by dust or other matter. But the effect I'm referring to is very different in appearance and causation. It cannot be photographed, and is evidently due to a limitation of the eye itself. Hermann von Helmholtz' book on Physiological Optics is almost a century old, but it is still one of the most useful compendia on the topic. In the English translation, a description of this effect is given in the section on monochromatic aberrations:

*With very intense light….as when the pinhole is illuminated by direct sunlight, the points of the star seem to merge together, while all around it an immense number of exceedingly fine, brilliantly colored, radiating lines form a sort of corona of much greater extent. The name hair corona will be used to distinguish this phenomenon from the star-shaped blurred image.* [6]

The rays also appear around automob, headlights, and around the filaments of flashlight bulbs. Walker mentions this as well [7]. He explains the effect as seen in photographs as being due to diffraction at the edge of the aperture. He cites J. R. Meyer-Arendt [8], which states that the effect in the human eye is due to diffraction at the irregular edge of the human pupil. Meyer-Arendt, in turn, gives no citation at all. Others hold that the fine lines of the solar rays are due to the radiate structure of the lens itself [9].

Which physical effect is responsible for these rays? Or is it due to both?

The diffraction from the edge of the pupil is one that, I must admit, occurred independently to me. I'm still not sure of the structure of the inner edge of the iris, but it seems likely to me that it must be something like a bag or a sweatshirt hood closed with a drawstring. When it contracts, the inner edge, like the top of a drawstring bag, ought to have a set of very fine yet irregular serrations. I have no assurance that this men picture is correct, and I have looked in vai. for corroboration from journal articles and from highly enlarge photographs of pupils. Certainly our experience with ubiquitous laboratory leaf-spring irises leads us to expect that physical irises are not perfectly circular. The curved-edge polygonal shape of laboratory apertures will produce diffraction images with spikes on them. The topic of far-field diffraction from polygonal apertures has been well-treated in the literature [10-15]. Diffraction by serrated-edge circular apertures, arguably a closer match for out case, has been modelled as well [16-18].

Helmholtz himself suggested that the rays might be due to "the minute indentations in the edge of the pupil". He noted that if an irregular aperture smaller than the pupil is placed before the eye one sees different rays, and that these rotate with the pupil [19]. M. Minnaert [20], in his classic book, noted that when the edge of the pupil is obscured by the eyelid, one sees longer rays in that direction, and that their direction normal to the eyelid at that point.

All of this is encouraging, but misses the directness of proof. Why not simply substitute a circular aperture known to be nearly

perfectly round? Perhaps Helmholtz had no good apertures, and had to make do with an irregular one. In any event, such apertures are easily available today. I found a 600 micron circular pinhole in our lab and held it up in front of my eye while looking at the bright filament of a Maglite flashlight.

The effect was dramatic. Although a little hunting in x and y were necessary, I was able to find a location where the Helmholtz hair corona completely disappeared. The radial filaments of light were replaced by dark circles, resembling Airy discs. This simple experiment seemed to be the most direct confirmation of the pupil-edge hypothesis. I saw no more filamentary rays. Nor did any of the others I asked to try the experiment, except one subject.

I'd still like to see a proper experimental proof of this, such as measuring the true shape of the pupillary aperture and using it to generate a diffraction pattern. But the experiments and papers listed give me confidence that almost all, if not truly all, of the "ray" effect is due to diffraction at the pupil's edge. Is there any significance to this?

I think that the appearance of these fine filamentary "hairy corona" rays has had a profound effect on the development of optics. I suspect that the image of rays extending outwards from a bright source suggested the idea of such light rays to early investigators of Optics -- Claudius Ptolemy, Alhazen, Descartes, and others, and that this gave us Geometrical Optics. (and later, Physical Optics).

The geometrical ray we are so familiar with from our introductory classes in optics is an abstraction. It can be approximated by the "pencil of light" one can obtain by letting sunlight in through a pinhole, but these could only be used for relatively short distances, and are weak. Even in works by the ancient Greek philosophers, however, light was thought to move in straight lines (although the direction as often reversed).

In reality, the ray represents the normal to the wavefront, and a more "natural" way to treat the propagation of light might be to propagate this wavefront through space. Even in works that have introduced me to the Huygens-Fresnel integral, however, the formulation has been in terms of rays from geometrical optics.

It's not easy to visualize an entire wavefront, but we can easily visulaize the progression of a single ray. This is precisely what Rene Descartes did when he produced his theory of the rainbow. He imagined a great many rays forming the wavefront, then traced the actual path of regularly spaced representatives from this vast assemblage of rays, noting how the rays from different points along the front were transformed by passage through the raindrop at different distances from the center. It wasn't feasible to treat the entire wavefront at once, but the ray optics approach allowed him to treat it piecemeal and get the same result.

In a way, this is parallel to the way the structure of the brain is studied. The tissue of the brain consists of closely-packed neurons, but that was not clear in the nineteenth century. Investigators wondered about the true structure of the brain, but were unable to untangle it, until Camillo Golgi was able to develop a stain for neurons that selectively affected only a few neurons, leaving the others uncolored. ✳

## References

1. http://www.nasa.gov/lb/audience/forkids/artsstories/AS_More_Sun_Drawings_by_NASAKids.html.
2. http://www.historical-reproductions.com/e-18.html.
3. http://rubens.anu.edu.au/htdocs/bytype/prints/brueghel/0001/110.JPG and http://rubens.anu.edu.au/htdocs/bytype/prints/brueghel/0001/111.JPG.
4. http://www.capetownskies.com/sunbeams.htm.
5. Jearl D. Walker The Flying Circus of Physics with Answers (1975/1977) John Wiley and Sons, p. 149.
6. Hermann von Helmholtz Helmholtz's Treatise on Physiological Optics, James P.C. Southall (ed.) Dover 1962 reprint of OSA 1924 translation of Third German edition p.129.
7. Walker, op. cit.,#5.97 on page 137.
8. Meyer-Aredt Introduction to Classical and Modern Optics (McGraw-Hill, 1972, p.3).
9. See, for example, W.D. Zoethout's Physiological Optics 3rd ed. Professional Press, Chicago 1939, pp. 95-6 and figure 66.
10. J. Komrska Optica Acta 19 (10) 807-16 1972.
11. J. Komrska Optica Acta 20 (7) 549-563 1973.
12. E. Hecht Amer. J. Phys. 40 (4) 571-576 1972.
13. Salvatore Ganci JOSA A 1 (5) 559-561 1984.
14. Winifred Sillitto JOSA 69 (5) 763-770 1979.
15. Richard C. Smith and James S. Marsh JOSA 64 (6) 798-803 1974.
16. B.K. Yap and S.D. Fantone JOSA 64 (7) 978-982 1974.
17. Nicholas George and G.M. Morris JOSA 76 (1) 6-17 1980.
18. Y. Kim, H. Grebel, and D.L. Jaggard JOSA A 8 (1) 20-26 1991.
19. Helmholtz op. cit. , p. 195.
20. M. Minnaert The Nature of Light and Color in the Open Air Dover Publ. 1954, pp. 94-95.

**Research Report**

# Photon Pairs from Multiexciton States in Single Semiconductor Nanocrystals

Brent R. Fisher, Jean-Michel Caruge, Moungi Bawendi

Department of Chemistry, MIT

The properties of a semiconductor nanocrystal (NC) differ significantly from those of the bulk. Due to confinement in all three directions, the electron and hole energy levels are quantized as if in a 3-d spherical square well into atomic-like states: "1S", "1P", "2S", etc. as shown in Fig. 1. Electrons and holes are created from the nanocrystal ground state by promoting a valence electron into the first available quantized electron state leaving behind a hole. The remaining 1e-1h configuration (or "exciton", X) can then recombine either nonradiatively or through the emission of a photon.
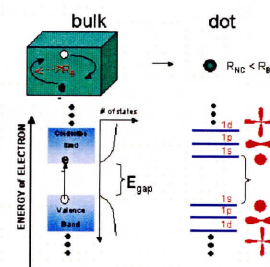


**Figure 1:** Schematic of the density of states in a bulk semiconductor and a 3-dimensionally confined semiconductor nanocrystal.

If the excitation is strong enough, multiple valence electrons can be sequentially promoted leading to 2e-2h (biexciton, BX), 3e-3h (triexciton, TX) and higher configurations. Electrons and holes then recombine pairwise: triexcitons decay to biexcitons, biexcitons to excitons, etc. Thus, it is possible to generate multiple emitted photons from a single pulse of excitation light. Moreover these photons could have knowledge of each other since they all derive from the same quantum system. For instance, the polarization of the biexcitonic photon might determine the polarization of the subsequent exciton photon. Such light sources have potential applications not only for fundamental quantum optics studies but also possibly in quantum computation and cryptography. It is thus important to characterize multiexciton emission from these dots, as well as demonstrate the creation and detection of multiexciton emission at the single dot level.

## Ensemble Measurements: the Auger Recombination Process

As a preliminary to single NC studies, we characterized the spectrum and dynamics of multiexciton emission from ensembles of NCs [1]. The sample used for all the studies in this report are core-shell CdSe-ZnS NCs with an approximately 5 nm radius core. Transient spectra from NC solutions were obtained on a streak camera after excitation at 400 nm by a frequency-doubled, amplified Ti:sapphire laser (1kHz). Figure 2b shows a typical result for high power excitation.
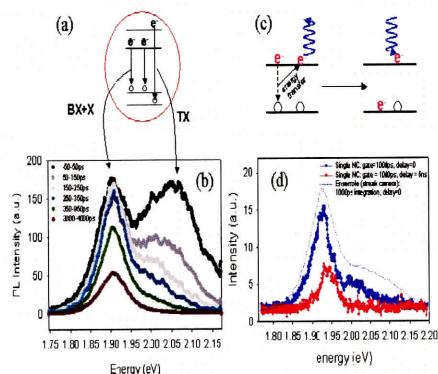


**Figure 2:** (a) Illustration of the electronic configuration of a triexciton. The third electron and hole reside in higher states than the first two. (b) Transient emission spectra at high power pulsed excitation from a solution of nanocrystals. (c) Schematic of the Auger process. First the exciton recombines giving its energy to a free electron. The "hot" electron then relaxes through intermediate states back to the lowest level. (d) Transient photoluminescence from a single nanocrystal.

The transient spectra show three principal features with distinct spectral and temporal signatures that turn on successively with increasing excitation power. Visible even at low intensities, the first feature, appearing at ~1.90 eV and decaying slowly over tens of nanoseconds, is assigned to the well-characterized [2,3] single exciton emission. As the power is increased, a much faster 790 ps - decay time component from the biexciton builds up on top of the first feature. The excitation power dependance matches what is expected, and spectral overlap is due to the second electron and hole occupying the same spatial orbitals as in the 1e-1h configuration. Unlike the exciton though, the biexciton emission decays very quickly, on the hundreds of picoseconds timescale, and has, in even the best of cases, a ten-fold reduced quantum yield [1].

A number of experimental [4,5] and theoretical [6] studies have helped pinpoint the nature of this additional non-radiative loss mechanism. The only types of non-radiative pathways available to the neutral exciton involve trapping or recombination at defect sites. In the presence of additional carriers, however, an electron-hole pair can recombine by simultaneously promoting an extra free electron high into the conduction band (or a free hole down into the valence band) in a single energy-conserving step, as in Fig. 2c. This Auger-like process is predicted to be quite fast [6] and has been shown to be consistent with size-dependance of the observed decay rate [4].

As the excitation intensity is further increased a third even faster emission band appears, blue-shifted at 2.05 eV. It is assigned to the triexciton. The multiplicity of free carriers now available to take up the energy from an electron-hole recombination suggests a very efficient Auger process, so the fast 270 ps decay is unsurprising. In contrast to the biexciton, the third electron cannot be accommodated into the lowest single particle spatial state due to Pauli exclusion and instead resides in the higher 1P state, hence the easily resolvable blue shift (Fig 2a). In fact, the TX emission energy tracks the 1P-1P single particle transition quite well [5].

These ensemble measurements were originally performed in the context of amplified spontaneous emission and lasing from close-packed NC and NC-doped titania films [5,7,8], an application that also depends crucially on multiexciton emission. For the purposes of the present work they provide a solid framework in which to understand the single molecule behavior and a number of important consistency checks to prove the generation of photon pairs and triples at the single nanocrystal level.

## Single Molecule Imaging: Multiexcitonic Emission

Single molecule imaging and spectroscopy has been a key tool for understanding nanocrystal emission. Usually blurred beyond recognition in the ensemble, the on-off fluorescence intermittency ("blinking") [9,10], sharp homogenous linewidths [11] and strong spectral diffusion [12] observed from single nanocrystals are not only interesting in their own right, but also explain otherwise mysterious ensemble behavior such as photo-darkening and photo-brightening in solutions [13] as well as the precise origin of the spectral breadth from ensemble emission [12]. The single molecule data presented in this work was obtained at room temperature in a home-built scanning confocal microscope using a high NA oil-immersion objective. All samples were NCs dispersed in a thin (~200 nm) layer of poly-(methylmethacrylate) and excited with 400nm pulses at 4.715 MHz from a frequency doubled Ti:sapphire oscillator.

Transient spectra from single NCs were recorded at high excitation intensities with a gated CCD camera (LaVision). The early time spectrum shows a pronounced blue-shifted contribution from the triexciton emission, demonstrating that multiexcitonic emission is indeed visible from single nanocrystals (Fig. 2d). Problems inherent to taking gated spectra of a fluctuating nanocrystal precluded a detailed analysis of the temporal profile, so we turned to a time correlated single photon counting (TCSPC) scheme to collect full photoluminescence decays.

In TCSPC, single emitted photons are detected with an avalanche photodiode and the time delay to the next excitation pulse is recorded with a suitable PC card (Picoquant). Fluorescence decay profiles are obtained from a histogram of the observed delay times. This detection system is thus largely immune to the nanocrystal blinking that complicates gated measurements. Figure 3a shows emission decays from a single NC at various powers: a slow exciton component dominates at low intensity while a faster, multiexcitonic, contribution builds in with higher power. The intensity dependence of the fast and slow weighting factors is consistent with a 4 level system model and a fit gives biexciton and triex-
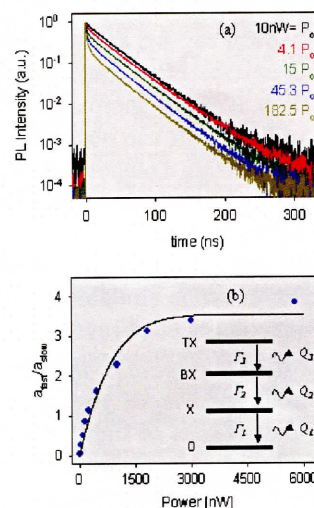
**Figure 3:** (a) Normalized photoluminescence decays from a single nanocrystal. Separate curves represent different excitation intensities. (b) Ratio of fast and slow decay component weights from the photoluminescence decay of a single nanocrystal as a function of excitation power. The line is a fit with the four level system model shown in the inset.

citon quantum yields consistent with the ensemble measurements (Fig 3b). Together with the gated CCD spectrum, this data establishes the observation of multiexcitons in single nanocrystals, but this is not enough. The potential applications demand at the very minimum that photon pairs (or triples) following single excitation pulses be demonstrated and characterized.

### Photon Cross-Correlation: Photon Pairs from Single Nanocrystals

Photon pairs from pulsed excitation were demonstrated in a photon cross-correlation experiment1 by detecting emission in a Hanbury-Brown-Twiss (HBT) geometry. A schematic of the experiment is shown in Fig 4. Collected emission photons pass through a 50/50 beamsplitter to either of 2 photodiodes: "start" or "stop". The times between the start and the next stop count are recorded with the same TCSPC PC card and summarized in a histogram. "Negative" times are allowed by cable delaying the stop signal. This technique has been fruitfully applied in a variety of single chromophore systems, ranging from nitrogen impurities in diamond [14] to multiexcitonic emission from self-assembled quantum dots [15].

The top graph in Fig 5a shows typical results with low intensity pulsed excitation. At these low powers only single excitons are prepared. After emission and detection with the "start" APD, the system must wait at least until the next excitation pulse (spaced 212 ns) to emit another photon. The missing peak at $\tau = 0$ is dramatic proof that the experiment probes only a single chromophore, while the shape of the side-peaks is closely related to the exponential distribution of delay times between emission and excitation from a single exciton (see Fig 3a).

An emerging peak with increasing excitation power is direct evidence of photon pair creation. Unlike the exciton, a system prepared in the biexciton configuration can emit two photons sequentially before the next pump pulse. At even higher intensities, triexcitons are prepared and a very sharp zero time component appears. This striking feature results from starting and stopping the counter with TX and BX photons: the time between them is necessarily very short because of the efficient Auger process.

The shape and power dependence of the photon cross-correlation histograms can be simulated with the four level system model and agrees well with our data (see Ref. 1 for details). In particular, the center-peak
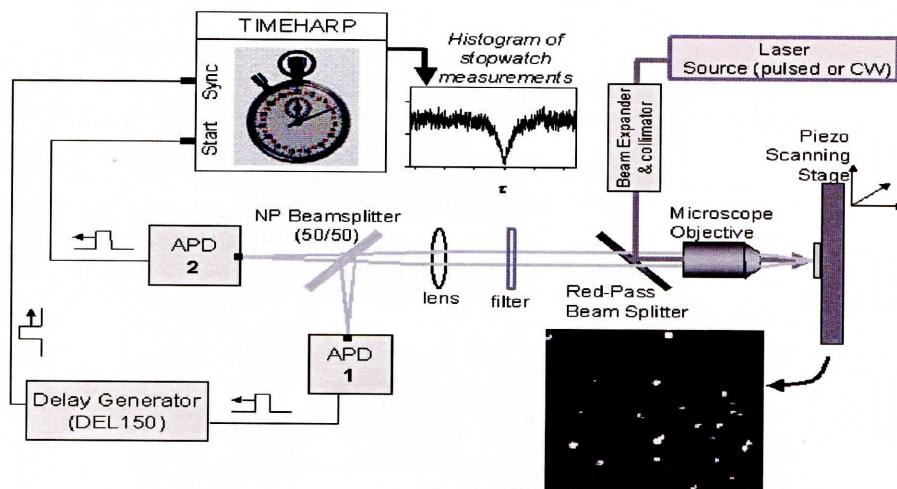


**Figure 4:** Schematic of the experimental setup for Hanbury-Brown-Twiss photon cross-correlation.
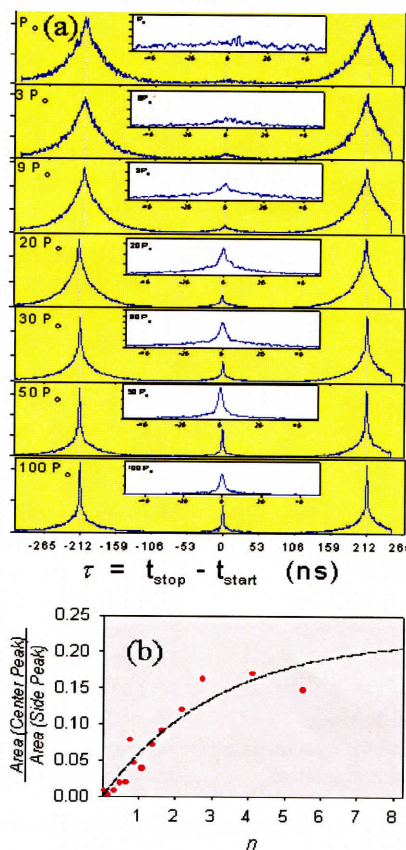


**Figure 5:** (a) Histogram of delay times between "start" and "stop" detected photons from a single nanocrystal under pulsed excitation. The excitation power is indicated in the upper left corner. Insets: close-ups of the zero time peak. (b) Ratio of central peak to side peak area plotted against the average number of e-h pairs created with each pulse. The dashed line is a calculated curve with no free parameters.

to side-peak area ratio versus excitation power closely tracks the calculated curve (Fig 5b). It should be noted that this calculation has no free parameters and instead uses values extracted from the ensemble and single dot experiments mentioned in previous sections.

### Conclusions

The spectral dynamics of multiexciton emission from ensemble and single nanocrystals has been characterized. Photon pairs originating from these multiexcitonic states in a single NC under pulsed illumination have been detected by single photon counting in a Hanbury-Brown-Twiss geometry. The reported data demonstrates that single colloidal nanocrystals are a source of nonclassical light. At a minimum, we hope this research will spur further fundamental research into the nature and correlations of photon pairs emitted from biexcitons.

### References

1. Fisher B. R. et al . Phys. Rev. Lett. 94 087403 (2005).
2. Schlegel G. et al. Phys. Rev. Lett. 88 137401 (2002).
3. Fisher B. R. et al. J. Phys. Chem. B. 108 143 (2004).
4. Klimov V. I. Et al. Science 287 1011 (2000).
5. Caruge J. M. et al. Phys. Rev. B 70, 085316 (2004).
6. Wang L. W. et al. Phys. Rev. Lett. 91 056404 (2003).
7. Klimov V. I. Et al. Science 290 314 (2000)
8. Sundar V.C., Eisler H.-J. and Bawendi M.G. Adv. Mater. 14 739 (2002).
9. Kuno M., et al. J. Chem. Phys. 115 1028 (2001).
10. Shimizu K. T. et al. Phys. Rev. B 63 205316 (2001).
11. Empedocles S. A., Norris D. J., and Bawendi M. G., Phys. Rev. Lett. 77 (1996).
12. Empedocles S. A. and Bawendi M. G., J. Phys. Chem. B 103 1826 (1999).
13. Chung I. And Bawendi M. G., Phys. Rev. B. 70 165304 (2004).
14. Kurtsiefer, C et al. Phys. Rev. Lett. 85 290 (2000).
15. Thompson, R. M. et al. Phys. Rev. B. 64 201302 (2001).
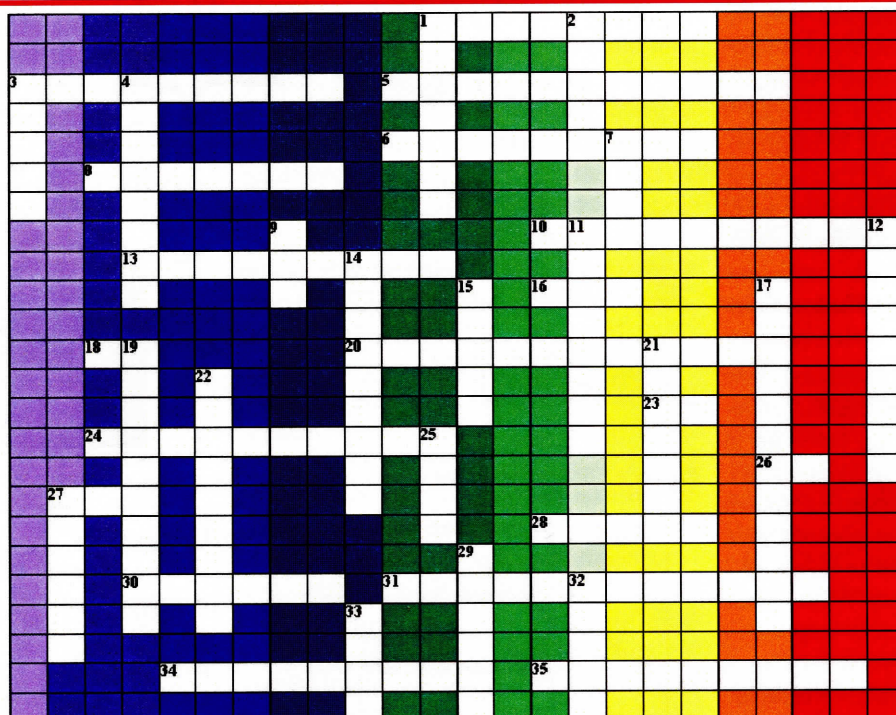
**Across**

1. heterogenous broadening
3. tiny wave
5. mercury lamps are commonly used for this
6. simplest is harmonic oscillator
8. Beer buddy
10. Rayleigh Criterion defines this
13. the main focus
16. doe, ray, …
18. $n_i \sin \theta_{max}$
20. light emitted at a different $\lambda$ than excitation
23. high spectral resolution light source
24. 30 – 300 GHz
26. analogous to the definition of decibel
27. sensitive detector
28. E-field induced splitting
30. $h\nu$
31. instrument built around 1 down
34. a diagram favorite of first-year spectroscopists
35. slow oscillation or constricted rotation

**Down**

1. highly dispersive element
2. characteristic blue to near-UV absorption band
3. laser predecessor
4. results in angular momentum
7. mass spectroscopy detects these
9. consists of an array of coupled capacitors
11. Einstein $A_{21}$ and $B_{21}$ coefficients describes this
12. the Nd in Nd:YAG
14. Raman scattering
15. examples include Johnson, shot
17. ♪ 'There will be an answer…' ♫
19. blue-shifted scattered light
21. originally short for excited dimer
22. examples include Glan-Thompson and Rochon
25. the first laser
27. packets of light
29. roughly 785 – 2400 nm
32. one divided by the other
33. an imaging element